*Supporting Information*

# Dynamical localization of a thylakoid membrane binding protein is required for acquisition of photosynthetic competency

Andrian Gutu[a,b,c], Frederick Chang[b], Erin K. O'Shea*[a,b,c]

[a] Howard Hughes Medical Institute, Harvard University Faculty of Arts and Sciences Center for Systems Biology, 52 Oxford Street, Cambridge, MA 02138, USA

[b] Department of Molecular and Cellular Biology, Harvard University Faculty of Arts and Sciences, 52 Oxford Street, Cambridge, MA 02138, USA

[c] Department of Chemistry and Chemical Biology, Harvard University Faculty of Arts and Sciences Center for Systems Biology, 52 Oxford Street, Cambridge, MA 02138, USA

*Corresponding author: Erin K. O'Shea, email: erin_oshea@harvard.edu

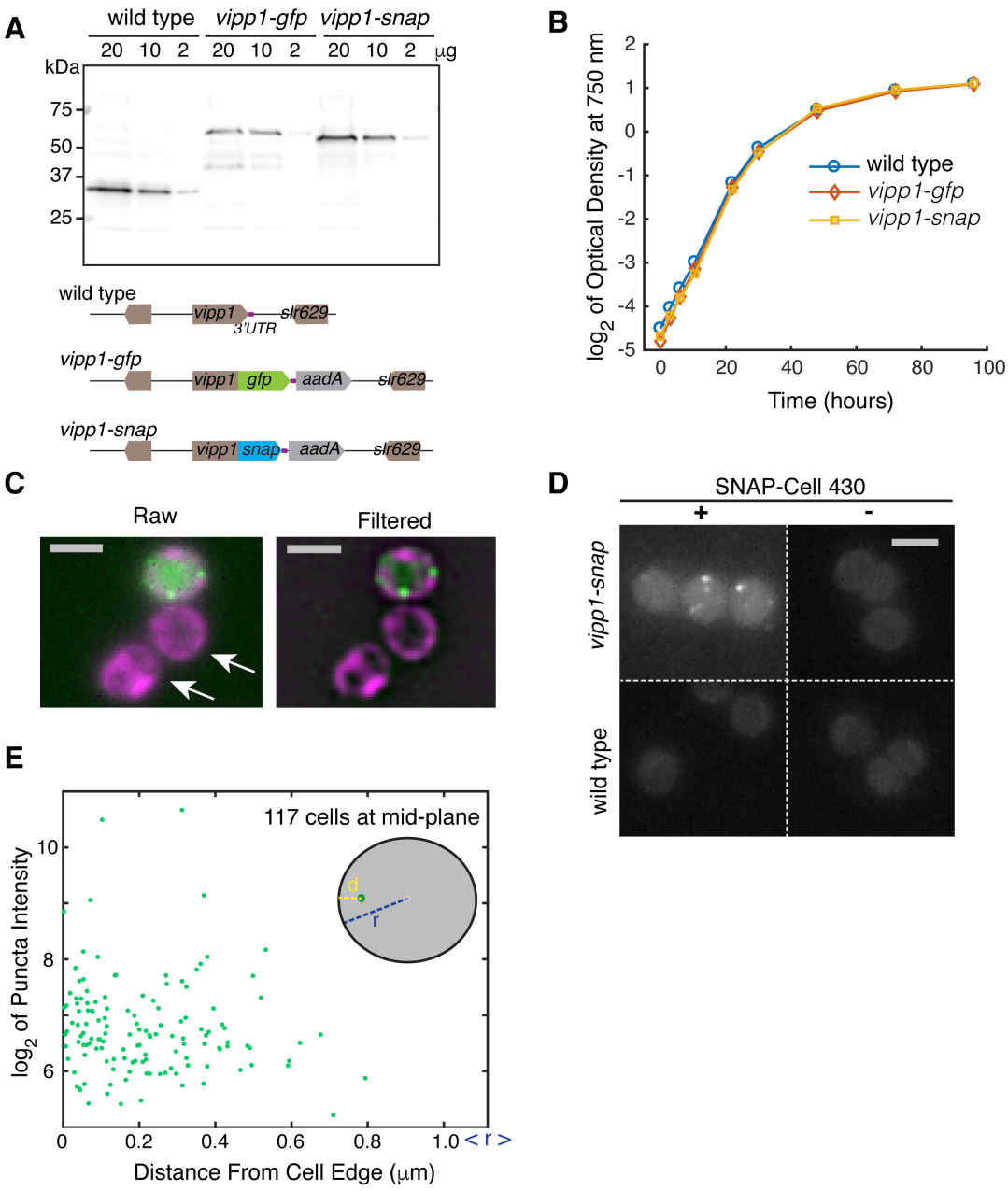


**Fig. S1.** Characterization of Vipp1 expression and cellular localization in strains with epitope-tagged versions of Vipp1. **A**) Immunodetection of Vipp1 in cell lysates obtained from wild type, *vipp1-gfp* and *vipp1-snap* cells. Western blotting was performed as previously described (Gutu and O'Shea, 2013). Anti-Vipp1 rabbit polyclonal antibodies raised against Vipp1 from *Chlamydomonas reinhardtii* (Agrisera AS06145) were used. Below are the diagrams of the Vipp1-tagged DNA constructs used in this study (see Methods). **B**) Growth of wild type, *vipp1-gfp* and *vipp1-snap* strains in liquid culture bubbled with a mix of air and 1% $CO_2$ at 100 µE $m^2$ $s^{-1}$ intensity light. **C**) Merged Vipp1 (green) and thylakoid (magenta) images of Maximum Z-Intensity Projections of a mix of *vipp1-gfp* and wild type cells (arrows) showing the difference in cytosolic signal intensity (i.e. diffuse fraction of Vipp1) between the two cell types. On the right,

an illustration of the filtering procedure (see Methods) used to enhance visualization of puncta and thylakoid features is shown. Scale Bar = 2 μm. **D**) Images of Maximum Z-Intensity Projections (raw epifluorescence) of wild type and *vipp1-snap* cells labeled with 5 μM SNAP-Cell 430 substrate (NEB S9109S) (after 20 min incubation in growth conditions) showing that Vipp1 puncta form independently of the GFP-tag. To facilitate comparison in signal intensity, the same grayscale contrast was applied to all four images. Scale bar = 2 μm. **E**) Intensities and distances of Vipp1 puncta relative to the cell edge. For any Vipp1 puncta found at or near the mid-Z plane of a cell, the intensity and the Euclidian distance (d) between its *xy* coordinates and the nearest point on the cell boundary edge obtained from segmentation in the brightfield channel was extracted and plotted. The <r> on the x-axis is the average cell radii of the 117 analyzed cells. Related to Fig. 1C for which the same dataset was used.

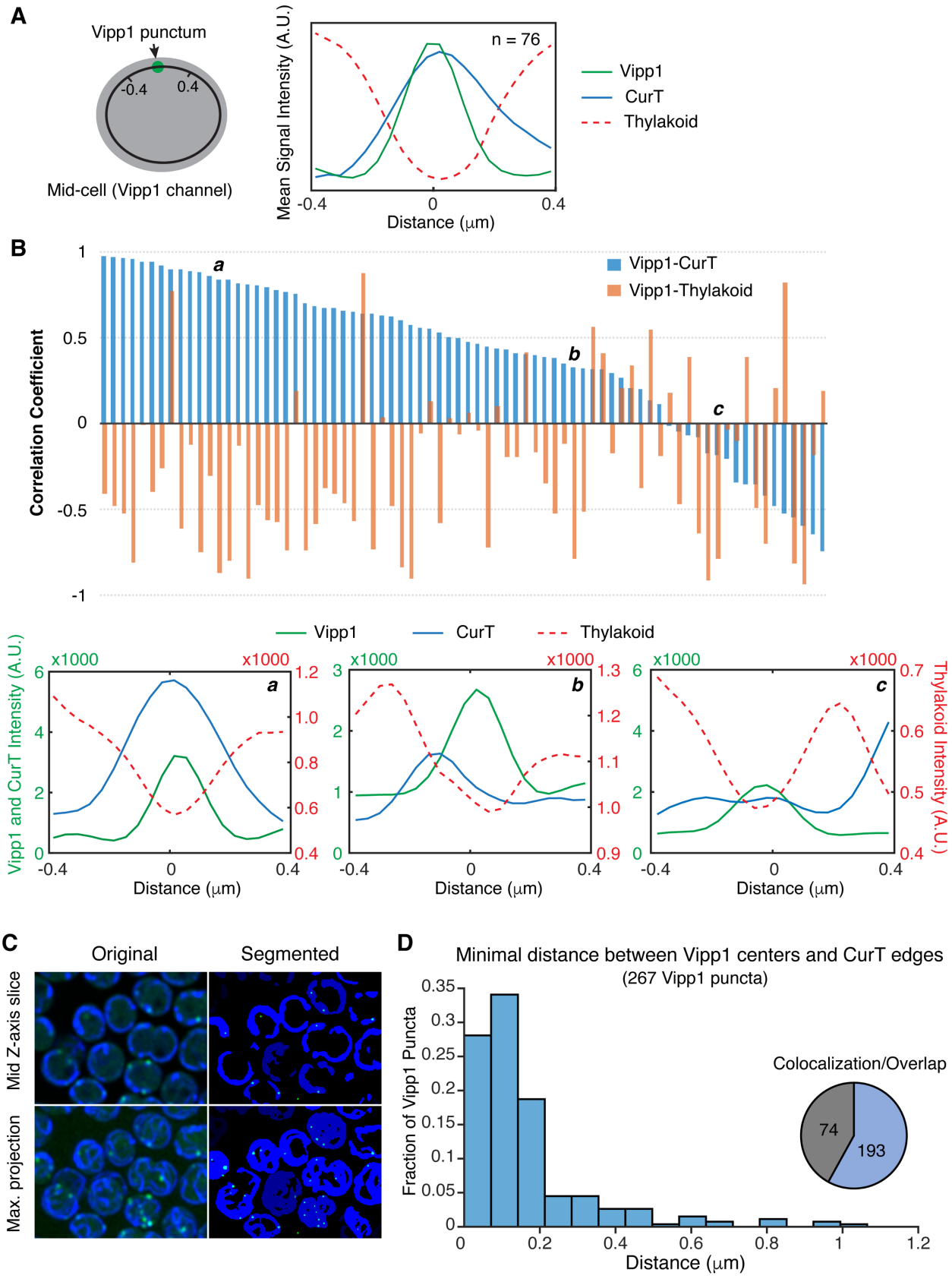
A
Vipp1 punctum
-0.4
0.4
Mid-cell (Vipp1 channel)
Mean Signal Intensity (A.U.)
n = 76
Vipp1
CurT
Thylakoid
-0.4
0
0.4
Distance (μm)
B
Correlation Coefficient
1
0.5
0
-0.5
-1
a
b
c
Vipp1-CurT
Vipp1-Thylakoid
Vipp1
CurT
Thylakoid
Vipp1 and CurT Intensity (A.U.)
Thylakoid Intensity (A.U.)
x1000
x1000
Distance (μm)
C
Original
Segmented
Mid Z-axis slice
Max. projection
D
Minimal distance between Vipp1 centers and CurT edges
(267 Vipp1 puncta)
Fraction of Vipp1 Puncta
0.35
0.3
0.25
0.2
0.15
0.1
0.05
0
0
0.2
0.4
0.6
0.8
1
1.2
Distance (μm)
Colocalization/Overlap
74
193

**Fig. S2**. Vipp1 puncta colocalize with CurT enrichments at thylakoid edges. A) **Left** - diagram illustrating how the arc line intensity profiles of Vipp1, CurT and thylakoid signals were obtained. The grey oval represents the cell at mid-Z plane. The green dot is a Vipp1 punctum localized at the same mid-Z plane. A manually traced circumferential (black circle) line parallel to the cell boundary and traversing the green Vipp1 punctum was used to extract the profile intensity in the Vipp1, CurT and thylakoid channels. For any given Vipp1 punctum identified as a peak in the profile (using Matlab's *peakfinder* function - see Methods), the intensities of the CurT and thylakoid signals were also collected for a 0.4 μm arc segment on either side of the Vipp1 peak (marked with a black notch). 76 arc segments (0.8 μm length) each centered on a given Vipp1 peak were extracted from 38 sets of intensity profiles that were obtained from 3D stacks of live-cells imaged in the Vipp1, CurT and thylakoid channels. The cells were imaged in superresolution mode on a confocal system equipped with the Airyscan detector (Zeiss LSM 880) (Korobchevskaya *et al.*, 2017) (see Methods). **Right** - average traces of Vipp1, CurT and thylakoid signals. **B)** Bar graph of the Pearson's correlation between Vipp1 and CurT, and Vipp1 and the thylakoid signals of each of the 76 datasets. In general, Vipp1 and CurT signals correlate positively, whereas Vipp1 and thylakoid signals correlate negatively (aggregated *p*-values: $1.22*10^{-6}$ and $5.57x10^{-62}$ respectively, null hypothesis tested being there is no relationship between the observed measurements). The weaker correlation values are obtained when the long axes of the thylakoid edges are quasi-parallel to the intensity profiles lines. Three correlation examples (labeled ***a, b*** and ***c*** in the bar plot) of intensity profiles are shown in bellow**. C**) Object-based colocalization analysis of Vipp1 puncta with the CurT enrichments. Example of Airyscan merged images of Vipp1 (green) and CurT (blue) channels and the corresponding segmentation masks obtained by iterative thresholding of the 3D stacks as implemented in the 3D ImageJ Suite plugin (Ollion *et al.*, 2013). Both mid Z-slice and Maximum Intensity Projection along the Z axis are shown. **D**) Histogram of the distance distribution of each Vipp1 punctum to its most adjacent CurT object (Vipp1 puncta centers to CurT object edges). 267 Vipp1 puncta obtained from an image stack containing ~70 cells were analyzed. Note that this analysis includes all distances regardless if the Vipp1 centers are "inside" or "outside" of the CurT objects. The majority of the distances between Vipp1 puncta and CurT edges fall under the optical resolution limit afforded by the Airyscan confocal imaging system (140 nm lateral and 400 nm axial). Inset pie chart shows how many of the Vipp1 puncta volumes overlap (in cyan) with the CurT objects.

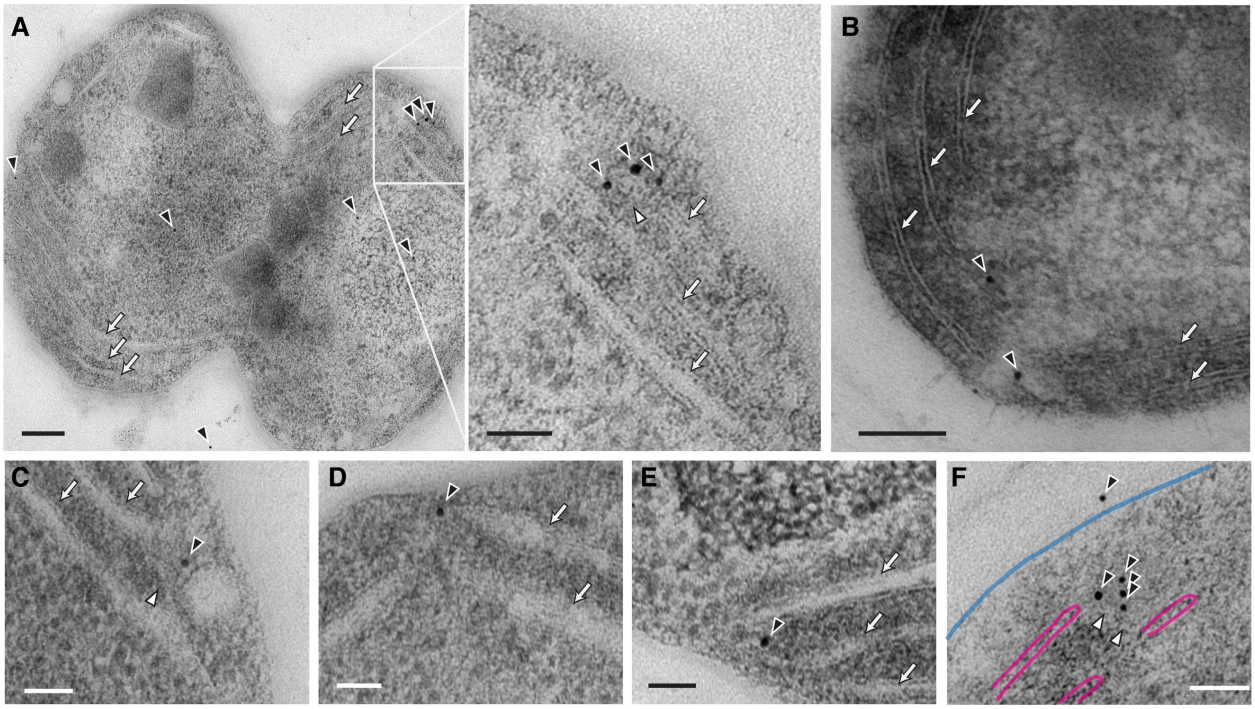


**Fig. S3.** Detection of Vipp1-GFP by immuno-electron microscopy. Examples of Vipp1-GFP staining (black arrowheads) in cell sections obtained from *vipp1-gfp* strain. The thylakoid sheets (open arrows) run parallel to the plasma membrane forming several peripheral stacks per cell. The majority of the gold stain observed tend to localize at thylakoid edges which appear as tips in 2D images. Occasional ring-like structures (white arrowheads) of 30-35 nm in diameter could be observed at or near the gold particles at these regions (**A, C** and **F**). The ring-like structures at these sites are reminiscent of the previously described thylakoid centers (van de Meene *et al.*, 2006). Plasma and thylakoid membranes in panel **F** are indicated with cyan and magenta overlays. **A-B**: scale bar = 100 nm (**A** inset panel: scale bar = 50 nm). **C-F**: scale bar = 50 nm.

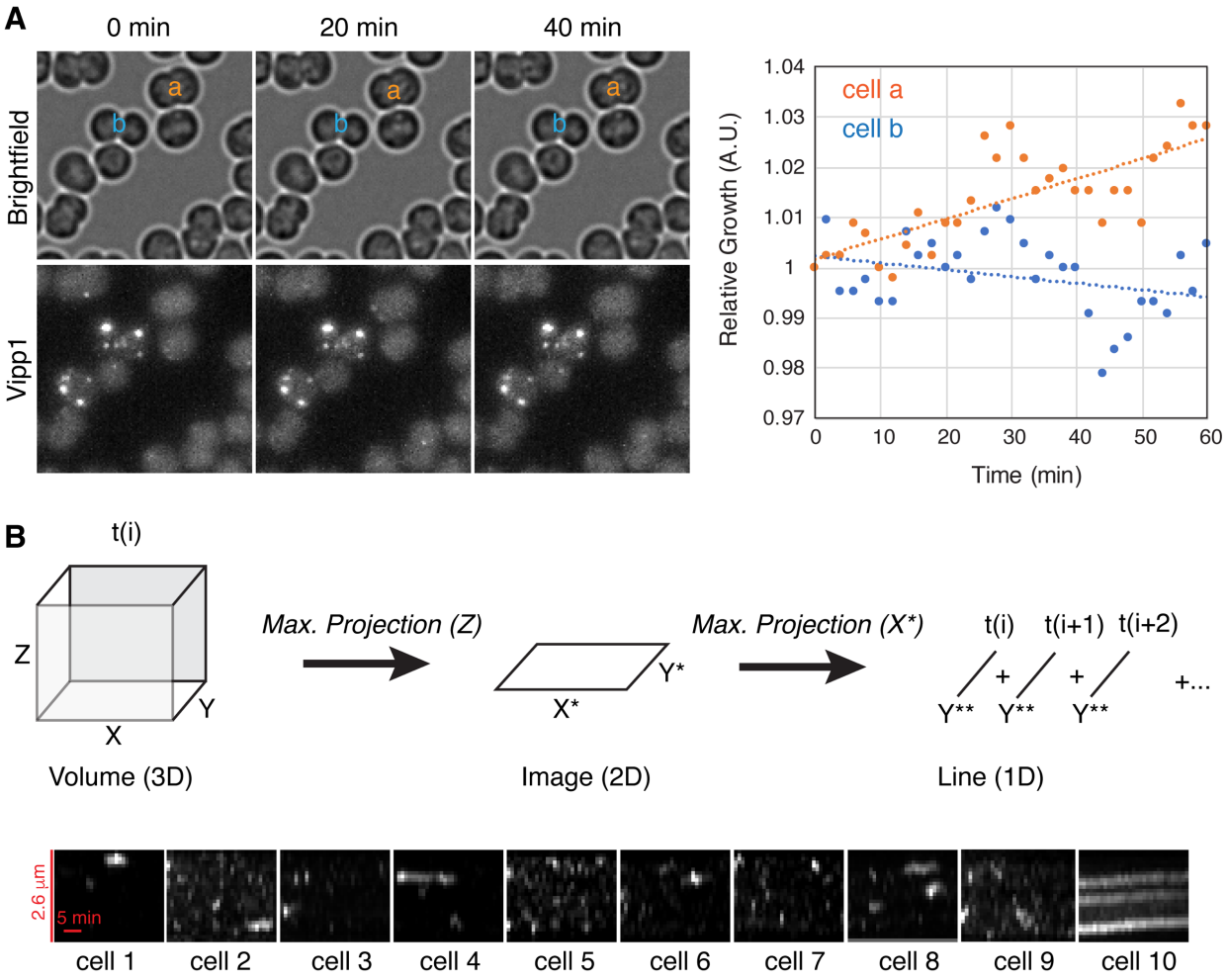


**Fig. S4.** Punctuated dynamics of Vipp1 is a hallmark of all growing cells. **A**) **Left** - montage of a field of view of cells imaged in timelapse mode in the brightfield and Vipp1 channels (Maximum Intensity Projections of raw epifluorescent 3D stacks - 8Z steps spaced every 280 nm) showing rare non-growing cells (see cell labeled "b") in which Vipp1 exists predominantly as bright and long-loved puncta as opposed to neighbouring growing cells in which Vipp1 puncta are dimmer and transient (see cell labeled "a"). Right - quantification of cell growth (as normalized cell areas relative to time 0) of cells "a" and "b" indicated in the montage on the left. Cell area measurements were extracted from automatic segmentation masks performed on the brightfield 3D stacks (see Methods). Cells were grown in light under an agarose pad, directly on the microscope stage and imaged every 2 min. Dotted trend lines represent least-square regressions of the raw measurements. The fraction of such non-growing cells is increased in samples obtained from older or stationary phase cultures. **B**) To better visualize the formation and number of Vipp1 puncta over time of a given cell imaged in time-lapse mode, we made kymograms from 3D stacks of individual cells by two successive dimension reductions. First, a 2D image of Maximum Z-intensity Projection of a given cell was obtained, then the *x*-dimension was maximum projected onto the *y*-axis, which was eventually concatenated in a time series to make the kymogram. Here we show kymograms obtained from 10 representative cells in the Vipp1 channel (filtered) collected every 1 min for 30 min (8 Z-steps spaced at every 280 nm).

Vipp1 puncta number and dynamics vary slightly from cell to cell - lasting generally 1-2 min. Occasionally (as also shown in panel A), we observed Vipp1 puncta failing to disassemble and slowly losing intensity due to photobleaching but invariably they would occur in a non-growing cell (for example, cell 10).

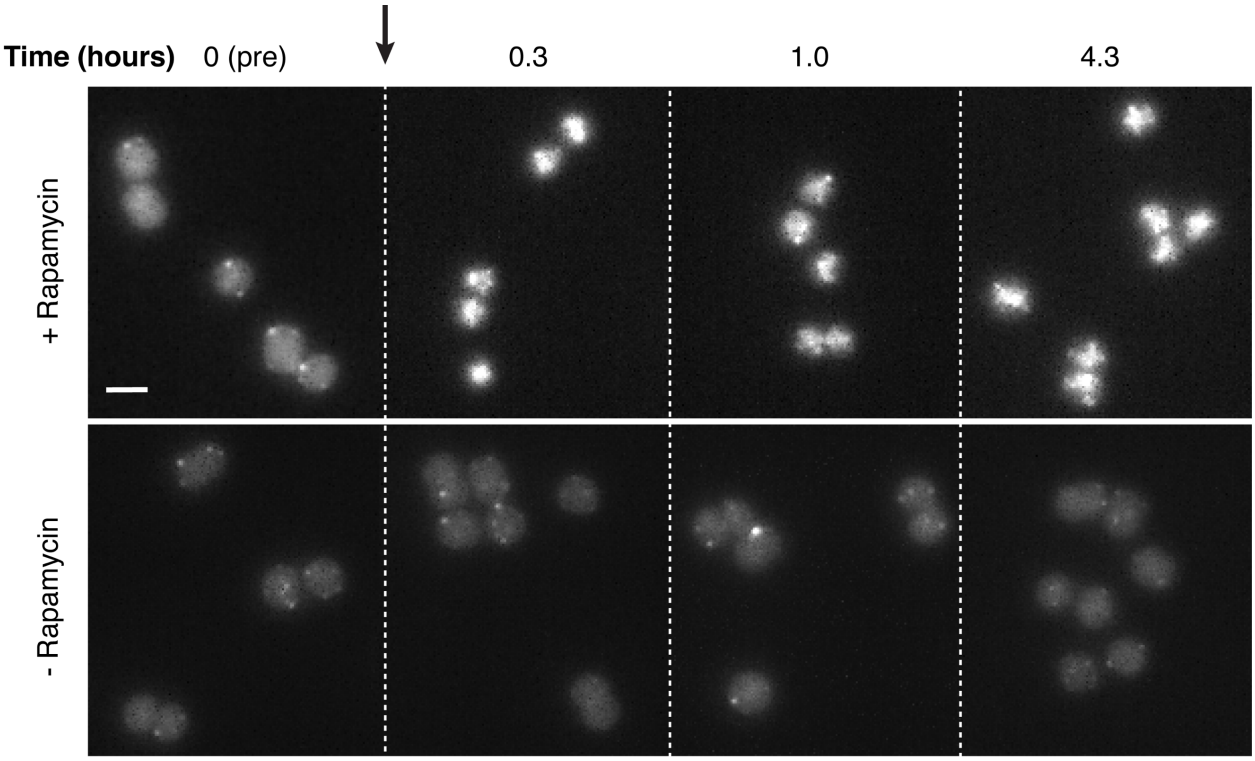


**Fig. S5.** Time-course of rapamycin-induced Vipp1 relocalization. Maximum Z-Intensity Projection images of cells expressing all the components of the anchor-away system and taken from a log-phase culture bubbled with 1% air-$CO_2$ mix at 100 µE µE $m^2$ $s^{-1}$ light intensity at different times before and after addition of 20 µM rapamycin or solvent (dimethyl sulfoxide) alone showing that relocalization of Vipp1 to the nucleoid at the cell centers is rapid, effective and stable for at least 4-5 hours. The same grayscale contrast was applied to all panels within each condition.

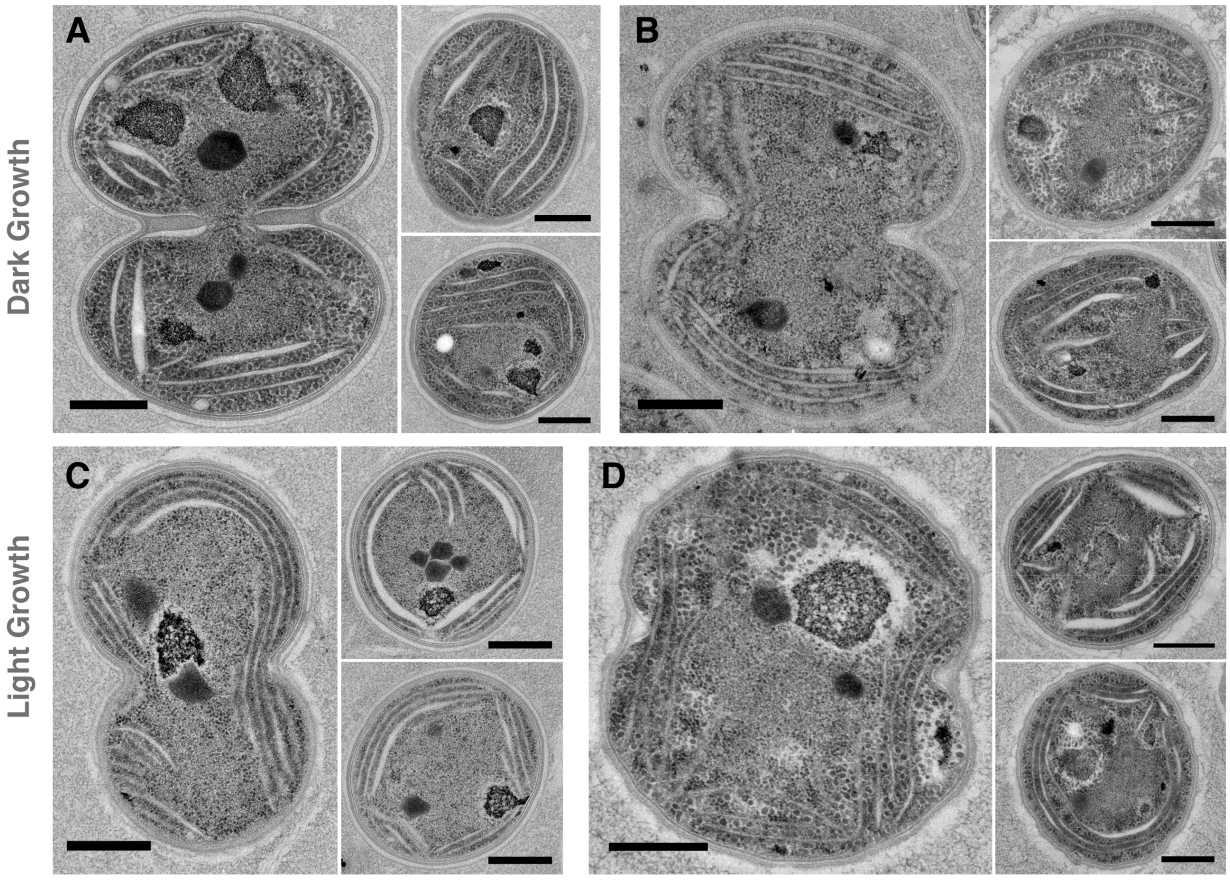


**Fig. S6.** Representative transmission electron microscopy images of dark- and light-grown cells expressing all the components of the anchor-away system after 48 hours of growth in darkness or in light in the absence or presence of 20 μM rapamycin. Dark-grown cells obtained by culturing the cells for 144 hours in darkness in the presence of glucose with brief exposures to activating light (see Methods) were diluted to an $OD_{750}$ of 0.1 in glucose-containing media and to which either dimethyl sulfoxide solvent (**A**) or 20 μM rapamycin dissolved in dimethyl sulfoxide was added (**B**) and further grown in complete darkness for 48 hours. Light-grown cells obtained from a log-growing culture were similarly diluted to an $OD_{750}$ of 0.1 in media with no glucose to which dimethyl sulfoxide alone (**C**) or 20 μM rapamycin in dimethyl sulfoxide (**D**) was added and grown in light for 48 hours. The overall morphology of the thylakoid stacks in rapamycin-treated cells is similar to that of the control cells. Scale bars = 0.5 μm.

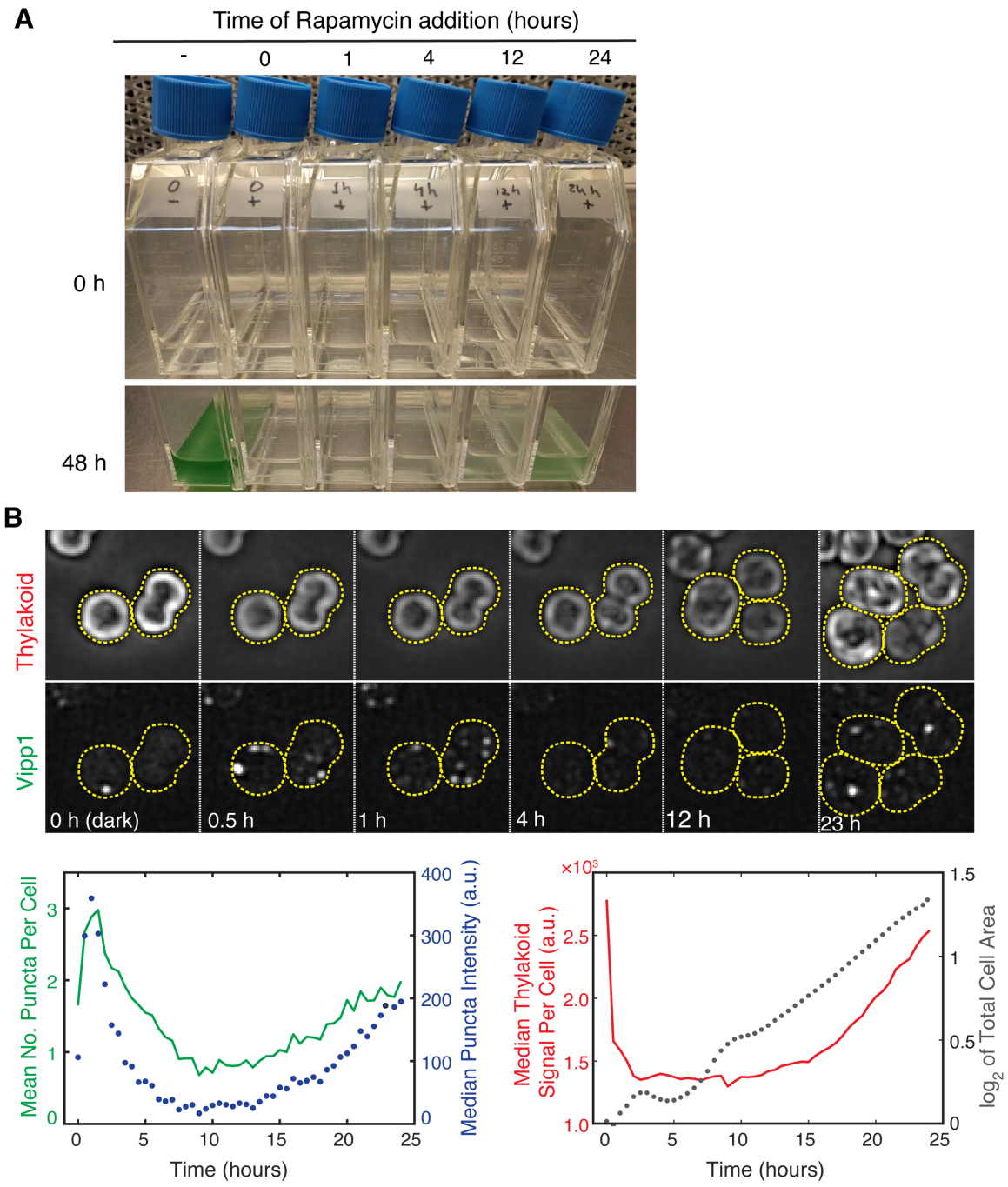


**Fig. S7.** The early stages of *Dark-to-Light Transition* are more prone to the effect of Vipp1 perturbation. **A**) Delaying Vipp1 relocalization to a later time during the *Dark-to-Light Transition* lessens the impact of the perturbation on growth – as evidenced by the increased pigmentation (i.e. growth) of cultures labeled 12 and 24 h. **B**) Vipp1 undergoes a burst in the rate of puncta formation in the early stages of the *Dark-to-Light Transition*. **Top -** selected images from a time-lapse montage of dark-grown *vipp1-gfp* cells transitioning to *Light Growth*. Maximum Z-Intensity Projections of 3D filtered stacks in the thylakoid and Vipp1 channels are shown. The same grayscale contrast was applied to the entire montage within each channel. **Bottom** - quantification of Vipp1 puncta number per cell, Vipp1 puncta intensities, total

thylakoid signal per cell and total cell area extracted from brightfield segmentation masks over time (every 30 min for 24 h) from a field ~260 starting *vipp1-gfp* cells. At time 0 h, before light is turned on, thylakoid auto-fluorescence per cell is high, likely because the existing photosynthetic pigments residing in the thylakoid membranes are uncoupled from photochemical reactions (hence more fluorescent). In growing photosynthetic light, total thylakoid signal per cell is relatively flat early on and starts accumulating after ~12 hours as the cells increase their thylakoid content and acclimate fully to the photosynthetic lifestyle. The initial dip in total cell area reflects the shrinkage of a small fraction of cells that fail to grow. For a full movie of a representative group of cells - see Video S6.

**Video S1.** 3D rendering of a live cell expressing Vipp1-GFP and CurT-mTurquoise2 based on an image stack obtained by Airyscan imaging. Vipp1 signal was thresholded to isolate out the Vipp1 puncta (green), which colocalize with the CurT enrichments (blue) situated the edge of thylakoid sheets (red). The movie was created using a modified version of the 5D renderer used in (Wait *et al.*, 2014). Scale bar = 1 μm.

**Video S2.** Vipp1 puncta are short-lived and form in all growing cells. Time-lapse imaging (every 2 min for a total of 60 min) of *vipp1-gfp* cells growing photosynthetically directly on the microscope stage. Maximum Z intensity projections (8-Z slices spaced at 280 nm) of raw epifluorescent images in the Vipp1 channel are shown. Scale bar = 2 μm.

**Video S3.** Majority of Vipp1 puncta appear and disappear at the cell periphery on a timescale ~1-2 min. Time-lapse imaging (every 30 sec for 10 min) of Vipp1 (left) and thylakoid (middle) channels of a group of photosynthetically growing cells. Merged filtered images of the middle Z-planes are shown. The arrow indicates an individual of Vipp1 punctum assembling and disassembling over time. Related to Fig. 3A.

**Video S4.** Vipp1 puncta have limited mobility. Continuous imaging in the Vipp1 channel (every 81 milliseconds for 8 sec) at mid-Z plane. The images were first bleach-corrected by histogram matching and then Laplacian-filtered to enhance visualization of Vipp1 puncta and cell edges. Related to Fig. 3C.

**Video S5.** Vipp1 relocalization during the *Dark-to-Light Transition* induces a severe growth defect. Timelapse movie (every 20 min for 24 h) of a mix of *vipp1-gfp-fkbp12* cells - with or without the HU-FRB anchor - transitioning from dark to light and to which 20 mM rapamycin was added after the first timepoint to induce Vipp1 relocalization. Maximum Z-Intensity Projections (10 Z-steps) of raw epifluorescent images in the thylakoid (left), Vipp1 (middle) and brightfield (right) channels are shown. The photosynthetic light (100 $\mu E\ m^2\ s^{-1}$) was turned on after the first timepoint. The cells in the which the Vipp1 signal coalesced at cell center (i.e. cells expressing the HU-FRB anchor) fail to grow or grow slower than the cells in which Vipp1 remains diffuse with occasional peripheral puncta (no HU-FRB anchor). Related to Fig. 5C.

**Video S6.** The early stages of the *Dark-to-Light Transition* are marked by a burst of Vipp1 puncta formation. Time-lapse movie of *vipp1-gfp* cells transitioning from *Dark* to *Light* growth. Dark-grown cells were placed under an agarose pad prepared with glucose-free media and imaged every 30 min for 24 h in brightfield, thylakoid and Vipp1 channels. Photosynthetic growth light was turned on after the first timepoint. Filtered Maximum Z-Intensity Projections (9 Z-steps) are shown for the thylakoid (left) and Vipp1 (right) channel. The linear grayscale contrast remained unchanged for the entire time series within each channel. Related to Fig. S7B.